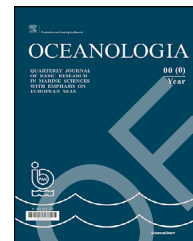


Available online at www.sciencedirect.com

ScienceDirect

journal homepage: www.journals.elsevier.com/oceanologia

ORIGINAL RESEARCH ARTICLE

Spatial variability of summer hydrography in the central Arabian Gulf

Elnaiem Ali Elobaid*, Ebrahim M.A.S. Al-Ansari, Oguz Yigiterhan, Valliyil Mohammed Aboobacker, Ponnumony Vethamony

Environmental Science Center (ESC), Qatar University, Doha, Qatar

Received 27 April 2021; accepted 16 September 2021

Available online xxx

KEYWORDS

Arabian Gulf;
Exclusive Economic
Zone (EEZ) of Qatar;
Physicochemical
parameters;
Water masses;
Stratification

Abstract The Arabian Gulf is a very significant ocean body, which hosts more than 55% of the oil reserves of the world and produces about 30% of the total production, and thus, it is likely to face high risk and adverse problems by the intensified environmental stressors and severe climatic changes. Therefore, understanding the hydrography of the Gulf is very essential to identify various marine environmental issues and subsequently, developing marine protection and management plans. In this study, hydrography data collected at 11 stations along 3 linear transects in the early summer of 2016 were analyzed. The physicochemical parameters exhibited apparent variations along each transect, both laterally and vertically, connected to stratification, formation of different water masses and excessive heating. The temperature and salinity decreased laterally from nearshore to offshore, while layered density structures were identified in the offshore regions. The pH, dissolved oxygen (DO) and chlorophyll fluorescence (Fo) exhibited distinct horizontal and vertical variations. The observed pH is within the normal ranges, indicating that seawater acidification may not be a threat. The highest DO (6.13–8.37 mg/l) was observed in a layer of 24–36 m water depth in the deeper regions of the central transect.

© 2021 Institute of Oceanology of the Polish Academy of Sciences. Production and hosting by Elsevier B.V. This is an open access article under the CC BY-NC-ND license (<http://creativecommons.org/licenses/by-nc-nd/4.0/>).

1. Introduction

The Arabian/Persian Gulf (hereafter “Gulf”) is a significant pathway from regional and international perspectives, hosting more than 55% of the oil reserves of the world and producing about 30% of the total world oil production (BP, 2011; Soliman et al., 2019). Thus, the Gulf is likely to face high risk and adverse environmental problems due to intensified natural and anthropogenic stressors in addition to climate change effects. The semi-enclosed Gulf is a western arm

* Corresponding author at: Environmental Science Center (ESC), Qatar University, P.O. Box 2713, Doha, Qatar.

E-mail addresses: elnaiemali123@gmail.com, elnaiem@qu.edu.qa (E.A. Elobaid).

Peer review under the responsibility of the Institute of Oceanology of the Polish Academy of Sciences.



Production and hosting by Elsevier

<https://doi.org/10.1016/j.oceano.2021.09.003>

0078-3234/© 2021 Institute of Oceanology of the Polish Academy of Sciences. Production and hosting by Elsevier B.V. This is an open access article under the CC BY-NC-ND license (<http://creativecommons.org/licenses/by-nc-nd/4.0/>).

Please cite this article as: E.A. Elobaid, E.M.A.S. Al-Ansari, O. Yigiterhan et al., Spatial variability of summer hydrography in the central Arabian Gulf, Oceanologia, <https://doi.org/10.1016/j.oceano.2021.09.003>

of the Indian Ocean, covering an area of $\approx 233,100 \text{ km}^2$, length of $\approx 1,000 \text{ km}$, the maximum width of $\approx 338 \text{ km}$, with an average depth of about 36 m (Kampf and Sadri-nasab, 2006). This unique physical setting extends within the most saline hyper-arid climate zone of the Arabian Peninsula desert belt, situated within the photic zone, as one of the most saline and hottest water bodies (Sheppard, 1993). In general, the Gulf is characterized by a tidal range of more than 1 m everywhere, with diurnal and semi-diurnal oscillations. The central Gulf waters are characterized by high salinity, which varies between 40 and 50 (Hunter, 1986). This is attributed to the high evaporation rate, which ranges from 144 to 500 cm/y (Brewer and Dyrssen, 1985). These combined factors make the system a reverse estuary and create an anticlockwise Mediterranean-like flow (Al-Majed et al., 2000; Reynolds, 1993; Yoshida et al., 1998).

The Gulf is subject to harsh natural and anthropogenic environmental stressors such as high salinity and extreme temperature during summer. The anthropogenic influence on salinity along the Arabian coast of the central part of the Gulf is mainly due to brine discharge from the desalination plants, resulting in adverse impacts on the marine ecosystem, particularly in the spatial distribution, diversity, existence and abundance of living organisms in this environment (Jones et al., 2002; Prasad et al., 2001; Privett, 1959; Soliman et al., 2019). Despite these harsh conditions, the Gulf hosts distinctive assemblage and habitats (Sheppard et al., 2010), but the natural environmental stressors have been reflected and witnessed by a decrease in the species richness levels (Price, 2002). The hypersalinity has adverse issues on the living organisms of the ecosystem (Joydas et al., 2015). For example, unhealthy benthic communities living in the hypersaline (salinity up to 63) region like the Gulf of Salwa are under high risk of radical natural stressors in comparison with the healthiest benthic communities living in relatively lower salinity regions of the Gulf (such as the east coast of Qatar and the coast of UAE). Moreover, the key physicochemical parameters of the water column, namely, temperature and salinity, influence the dissolution processes, affinity adsorption and mobility of pollutants in the marine environment (Ma et al., 2016; Soliman et al., 2019).

The small and limited freshwater input and high evaporation rate have influence and control on the circulation and water masses of the Gulf (Campos et al., 2020; John et al., 1990; Prasad et al., 2001; Reynolds, 1993), and hence the information on physical oceanographic parameters such as temperature, salinity and density is vital to analyze the horizontal and vertical distribution of the water masses and to assess the diffusive and advection transports within the water column (Al Azhar et al., 2016; Kampf and Sadri-nasab, 2006; Pous et al., 2015). The circulation characteristics are important to determine the distribution of sediments, dynamics of nutrients and fate of pollutants (Soliman et al., 2019). Beltagy (1983) reported that the main controlling factors of vertical and horizontal salinity distribution in the Gulf are higher rates of evaporation, seepage of fresh water, brine discharges and evaporitic deposits. The spatial distribution pattern of salinity and temperature have been investigated previously by several researchers (Beltagy, 1983; Emery, 1956; Kampf and Sadri-nasab, 2006; Reynolds, 2002;

Shepherd, 1993). They reported that the salinity decreases towards the offshore areas, and increases within the coastal areas and ports, whereas temperature decreases from the coastline towards the offshore and also decreases as depth increases.

A detailed understanding of spatial variability of physicochemical parameters is important to analyze the physical and biogeochemical interactions and their impact on the marine ecosystem of the central Gulf. There are very few studies in this part of the Gulf on the spatial variability of physical and biogeochemical parameters. The present study aims at understanding the spatial variability in the physicochemical parameters of the central Gulf by analyzing the measured hydrographic data during summer. The role of different water masses and seasonal stratification in the biogeochemical processes of Qatar's Exclusive Economic Zone (QEEZ) have been addressed. The study also explores the statistical relationship between various physicochemical key parameters.

The paper is organized as follows: Section 2 describes the area of study, Section 3 explains the data and methodology used, Section 4 explains the important results and their discussions, and Section 5 summarizes the major inferences.

2. Area of study

The Qatar Peninsula is situated in the central Gulf with an area of $11,437 \text{ km}^2$, centered at 25°N and 51°E . The EEZ of Qatar is located between the longitudes $51^\circ00'\text{E}$ and $52^\circ30'\text{E}$ and latitudes $24^\circ50'\text{N}$ and $26^\circ58'\text{N}$ (Figure 1), with an area of $35,000 \text{ km}^2$ (Al-Ansari, 2006). The winds are predominantly from the NW-N directional sector, where the highest wind speeds of the order of 22 m/s are due to shamal winds (Aboobacker et al., 2021a). The surface currents within the QEEZ are mainly wind-driven; however, the deeper regions are influenced by thermohaline circulation (Chao et al., 1992; Thoppil and Hogan, 2010). The physical processes such as circulation, eddy formation and sedimentation in the QEEZ are largely influenced by the geographical setting of the Qatar peninsula, which in turn influence the development/survival of the ecosystem (Al-Ansari, 2006).

In this study, we considered 3 major transects with a total of 11 stations. The transects are directed from the coastline towards the deep sea, more or less perpendicular to the coast as shown in Figure 1. The southern transect is about 110 km long, occupying three stations S2, S3 and S4; the central transect is about 100 km long with four stations C1, C2, C3 and C4; the northern transect is about 90 km long with four stations N1, N2, N3 and N4.

3. Data and methodology

The physicochemical parameters such as temperature (T), salinity (S), density (D), pH, dissolved oxygen (DO), chlorophyll fluorescence and the water column depth were measured using SeaBird-911plus CTD and auxiliary sensors, manufactured by Seabird Scientific Company and used onboard R.V Janan. Seasoft software was integrated to the CTD system for the simultaneous processing of the data. The verti-

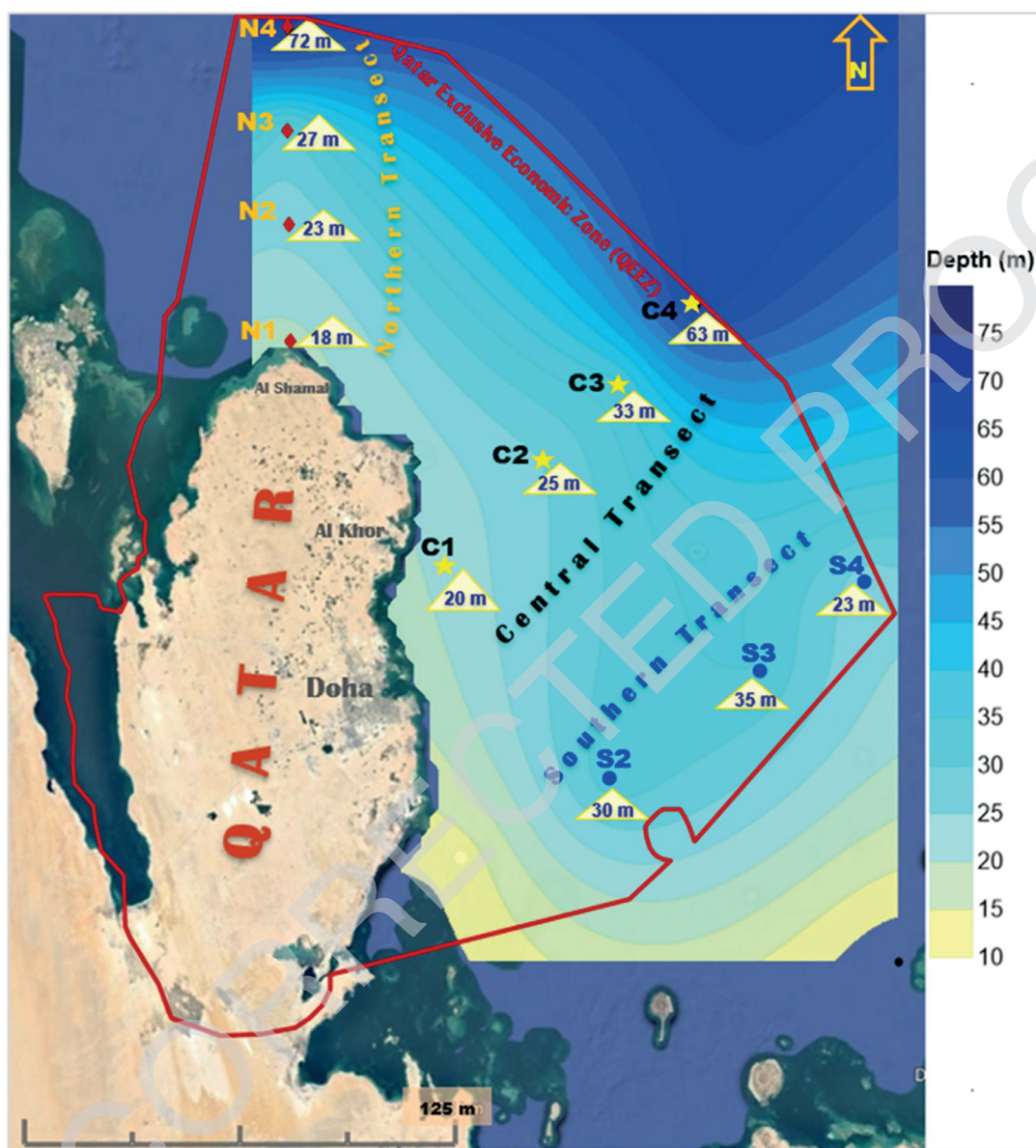


Figure 1 Area of study with sampling stations along the three transects together with generalized bathymetry (bathymetry data is retrieved from Ocean Data View). Depth, of each station measured using echo-sounder onboard RV Janan, is given inside the yellow triangle. Bathymetry contours are generated using Surfer software.

128 cal sampling frequency of the CTD was set to 1.0 m. The bin
 129 size was 1.0 m and the raw data was averaged over each bin.
 130 The accuracies of conductivity, temperature and pressure
 131 are ± 0.0003 S/m, $\pm 0.001^\circ$ and 0.015% of full-scale range,
 132 respectively. The potential density (σ_t), calculated using
 133 the formula described in Fofonoff and Millard (1983),
 134 was obtained from the CTD records.

135 The processed physicochemical parameters have been
 136 analyzed to derive their spatial variabilities. Ocean Data
 137 Viewer (ODV) software version 5.03 was used to create the
 138 2D profiles of temperature, salinity, density, pH, dissolved
 139 oxygen (DO), and fluorescence (Schlitzer, 2020). The Pear-
 140 son correlation matrix method was performed using SPSS
 141 version 25 to evaluate the statistical relationship between
 142 the physicochemical key parameters.

4. Results and discussion

143

4.1. Distribution of temperature, salinity and density

144

145

146 The distribution of physicochemical parameters in the Gulf
 147 is primarily controlled by the geographical settings, air-
 148 sea interactions and ocean processes (Figure S1). For in-
 149 stance, higher salinity is observed along the Arabian coast
 150 of the Gulf, where the evaporation is much higher (144
 151 cm/y) and the freshwater influx is very low ($1,456 \text{ m}^3/\text{s}$)
 152 (Reynolds, 1993). As a result, higher salinity water masses
 153 are formed in the southern coast of the Gulf (Al-Ansari, 2006
 154 and Rivers et al., 2019). In addition to natural processes, an-

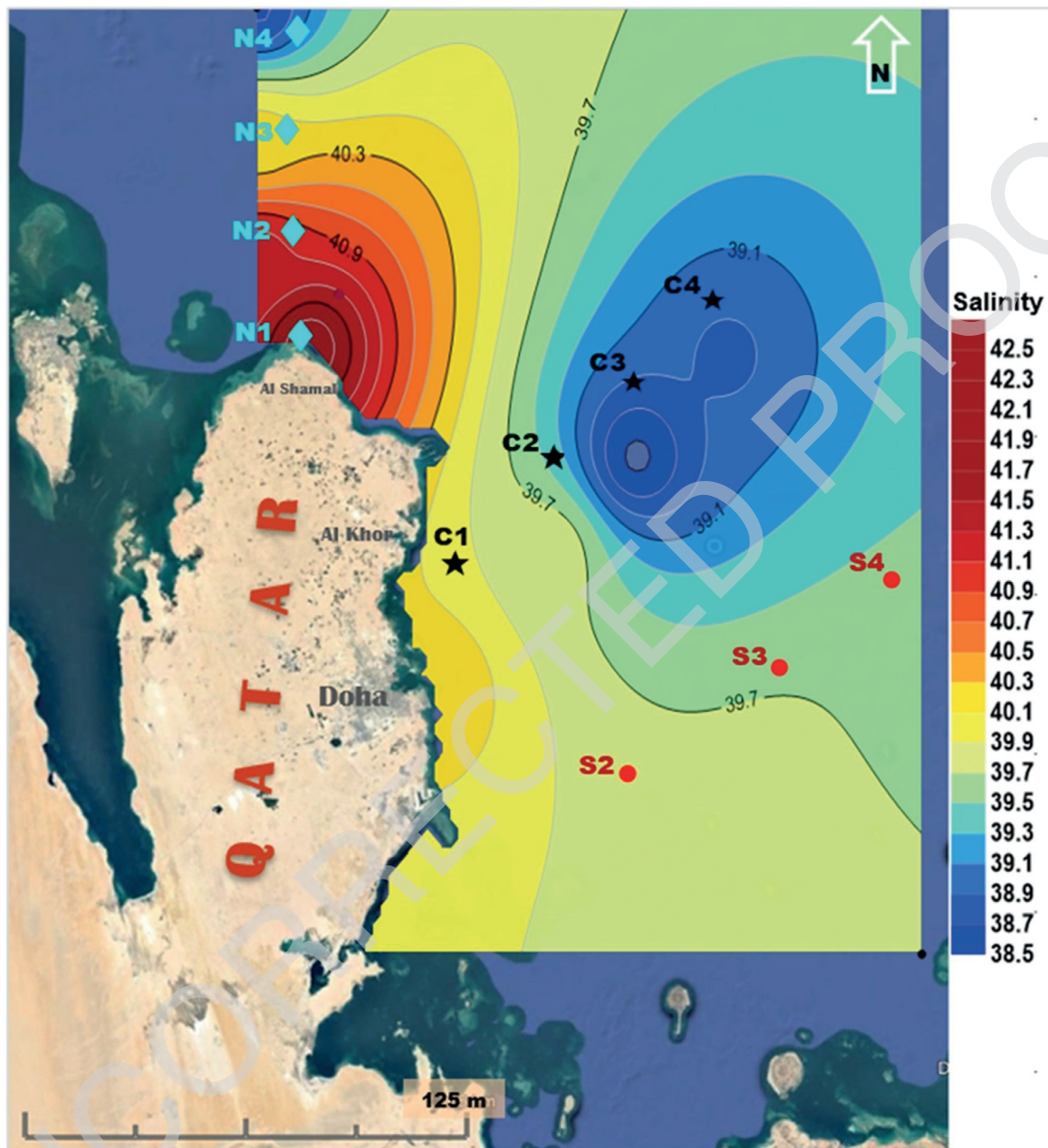


Figure 2 Generalized spatial contours of sea surface salinity (SSS) at 5 m depth derived from the CTD measurements along the three transects.

155 thropogenic forcing in the form of brine discharges from the
 156 desalination plants operated along the Arabian coasts may
 157 also add an accountable amount of salinity to the nearshore
 158 waters, although their impact in the deeper waters is not
 159 that significant (Ibrahim et al., 2020; Ibrahim and Eltahir,
 160 2019; Rakib et al., 2021). Our analysis shows that higher
 161 salinity in each transect is found in the nearshore sta-
 162 tions, and the salinity gradually decreases towards offshore
 163 as shown in the generalized spatial contour map (Figure 2).

164 A wedge-like intrusion of low saline water is visible in
 165 the offshore, deeper regions of the central transect, which
 166 is quite unique compared to the other two transects. This
 167 is in agreement with the pattern of low salinity intrusion
 168 identified from the Arabian Sea to the Gulf by Ghaemi et
 169 al. (2021). This is linked with the exchanges between the

170 Gulf of Oman and the Arabian Gulf, which are driven by the
 171 differences in sea surface heights of the two regions (Swift
 172 and Bower, 2003) and also due to baroclinic forcing devel-
 173 oped by the density gradients (Chao et al. 1992; Yao and
 174 Johns, 2010). The exchanges are intensified following an
 175 enhanced two-layer flow during late winter through early
 176 summer, whilst the flow diminishes during mid-summer to
 177 mid-winter (Vasou et al., 2020). Among the three transects,
 178 the highest salinity is found in the northern transect, and
 179 it could be attributed to the following reasons: (i) higher
 180 evaporation due to relatively stronger winds in the offshore
 181 region (deeper) compared to the nearshore region (shal-
 182 lower) (Aboobacker et al., 2021b), (ii) considerable heat-
 183 ing because of very shallow depths, (iii) advection of hy-
 184 persaline Gulf of Salwa Water (GSW) (Al-Ansari et al., 2015)

185 and (iv) dispersion of brine discharged from the desalina-
186 tion plants situated along the northeast coast of Qatar. The
187 higher evaporation along with dense water flow from the
188 northern Gulf has got prime importance in higher salinity
189 in the northern transect (Smith et al., 2007). Recent stud-
190 ies point out that the hypersalinity in the southwestern Gulf
191 at specific locations can also be attributed to the presence
192 of desalination plants (Ibrahim and Eltahir, 2019), though
193 the general surface circulation of the Gulf does not permit
194 building-up of salinity.

195 In the nearshore regions of the northern transect, tem-
196 perature, salinity and density are relatively higher com-
197 pared to the surface layer of other stations (Figure 3a1, a2,
198 a3). The temperature and salinity in the nearshore regions
199 are vertically homogeneous due to limited depths of the wa-
200 ter column, whereas they decrease from nearshore to off-
201 shore. In the offshore, there is a distinct vertical variabil-
202 ity in temperature and salinity, especially with substantially
203 low saline water in the surface layer and low temperature
204 in the bottom layer both leading to vertical stratification.
205 These differences are reflected in the density distribution
206 with distinct patterns, indicating the presence of two wa-
207 ter masses. Earlier studies indicate that the low salinity wa-
208 ter mass, Indian Ocean Surface Water (IOSW) intrudes up
209 to the central Gulf during summer (Kampf and Sadrinasab,
210 2006). Although similar features (salinity and density varia-
211 tions) are found in the central transect, more investigations
212 are needed to establish the intrusion of IOSW up to the east
213 coast of Qatar as the salinity differences obtained in this
214 study are relatively small. In addition, the sea surface tem-
215 perature (SST) has shown little variation from nearshore to
216 offshore (Figure 3b1, b2, b3), which is due to the excessive
217 surface heating distributed equally in the central Gulf dur-
218 ing summer compared to the other regions (Van Lavieren et
219 al., 2011). Interestingly, there is a sublayer of intermedi-
220 ate density, indicating the role of eddies in the central Gulf
221 (Reynolds, 1993). The low salinity surface water of the or-
222 der of 38.5–40.0 and 38.2–39.5 in the northern and central
223 transects, respectively point to the exchange of low salinity
224 water from the Sea of Oman to the offshore regions of QEEZ.
225 The region of influence of this low salinity surface water and
226 the dense bottom water is small in the southern transect as
227 identified by their minimal vertical variations (Figure 3c2,
228 c3). The vertical variation in temperature is also not signif-
229 icant in this transect (Figure 3c1).

230 The vertical variation in temperature, salinity and den-
231 sity is significant only in the deepest stations among all the
232 transects (Figures 4a, b, c). The temperature variations in
233 the northern, central and southern transects during early
234 summer are in the range of 19.9°–30.2°C, 20.2°–28.4°C and
235 26.8°–28.7°C, respectively (Table S1). The salinity varia-
236 tions in the above transects are 38.7–42.2, 38.5–40.9 and
237 39.6–40.1, respectively. Previous studies identified a signifi-
238 cantly higher salinity (above 44) along the nearshore regions
239 of Doha and Mesaieed, the central east coast of Qatar during
240 the summer of 2000 (Abdel-Moati and Al-Ansari, 2000; Rakib
241 et al., 2021). However, our present analysis does not repre-
242 sent these coastal stations as they are far from the transects
243 under consideration. It is worthy to note that the central
244 east coast of Qatar is housing several desalination plants,
245 which are discharging a high amount of brine into the sea.
246 In the GCC countries, for every 1 m³ fresh water produced,

2 m³ brine is generated and discharged into the Gulf (Sezer 247
et al., 2017). Brine can drop the level of DO in seawater 248
near desalination plants with "profound impacts" on benthic 249
biota such as shellfish and crabs on the seabed. The ambient 250
salinity in the vicinity of the outfalls might have increased 251
due to the hypersaline influx. A detailed investigation on the 252
cumulative impact of the discharged brine over a longer pe- 253
riod of time in the QEEZ is yet to be conducted to quantify 254
the anthropogenic influence on the hyper salinification of 255
the nearshore waters of the central east coast of Qatar. The 256
changes in salinities within the water mass is likely to affect 257
the growth of some of the marine organisms (Joydas et al., 258
2015). Consequently, brine discharges lead to negative eco- 259
logical impacts observable throughout the food chain in the 260
Gulf. 261

4.2. Water masses in the QEEZ 262

The water masses in the QEEZ have been determined by 263
analyzing the T-S diagram of each transect (Figure 5). The 264
Qatar Shallow Water (QSW) with the density between 24.98 265
and 27.55 kg/m³ has been identified at all the transects, 266
which is characterized by high temperature, low salinity and 267
low density (Figure 5a). The Qatar Deep Water (QDW) with 268
the density between 27.87 and 29.32 kg/m³ has been identi- 269
fied in the northern and central transects, which is charac- 270
terized by low temperature, high salinity and high density 271
(Figure 5b). Recently, Rakib et al. (2021) identified these 272
two water masses during the late summer (September 2014) 273
in a deep-water location, adjacent to the deepest station 274
in the central transect, but with an increased SST due to 275
seasonal transformation from early summer to late summer. 276
The Qatar Intermediate Water (QIW) with distinct values of 277
temperature, salinity and density has been observed in be- 278
tween QSW and QDW in the central transect (Figure 5c). This 279
is consistent with that identified from the measurements of 280
July 2000. 281

282 The physicochemical properties of the water masses 283
in the QEEZ, namely, Qatar Central Arabian Gulf Water 284
(QCAGW) during summer is quite different from those de- 285
rived for the water masses (listed in Table 1) at different 286
regions in the Gulf (Al-Said et al., 2018). Though the dis- 287
tinct variation in temperature is observed among all the 288
water masses, only in the QCAGW, wider variation is found. 289
The salinity difference in the Indian Ocean Surface Water 290
(IOSW) and Central Arabian Coastal Water (CACW) is rela- 291
tively small, while that in the QCAGW is relatively higher. DO 292
ranges widely in QCAGW compared to other water masses, 293
and pH has no significant variations among the water masses 294
in the Gulf.

4.3. Distribution of pH, dissolved oxygen and 295 fluorescence 296

The pH in each transect shows distinct variations horizon- 297
tally and vertically (Figure 6a1, b1, c1). Although small, the 298
variations in pH are consistent with the water mass distri- 299
butions, especially in the deep-water regions of northern 300
and central transects. In the central transect, the highest 301
pH (~8.2) is in the subsurface layer, which clearly depicts 302
the presence of QIW. The variations in pH among all the 303

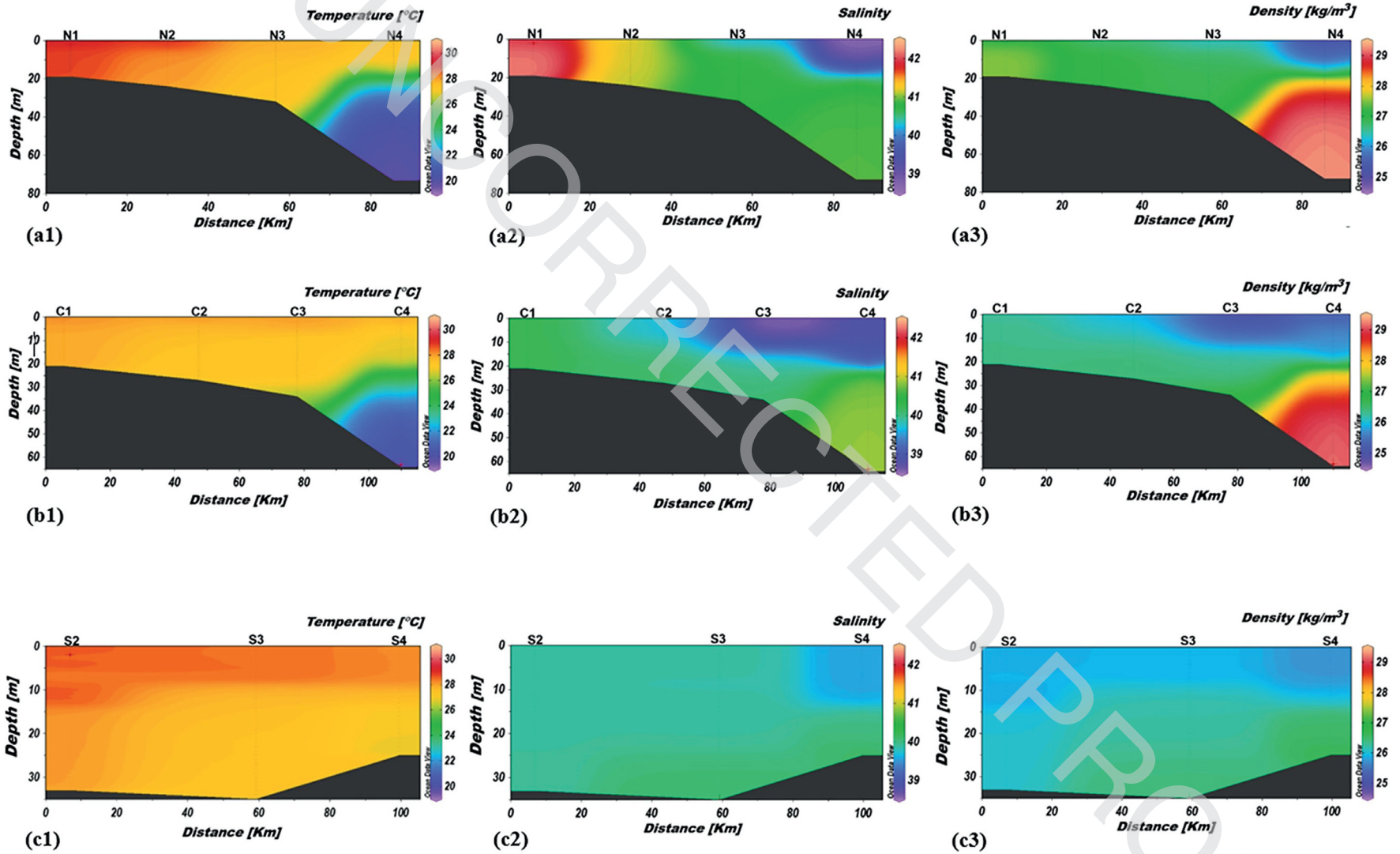


Figure 3 2D profiles of the measured temperature (a1, b1 and c1), salinity (a2, b2, c2) and density (a3, b3, c3) along the northern (a), central (b) and southern (c) transects. The plots are made using Ocean Data View Software, Version 5.03, (Schlitzer, 2020).

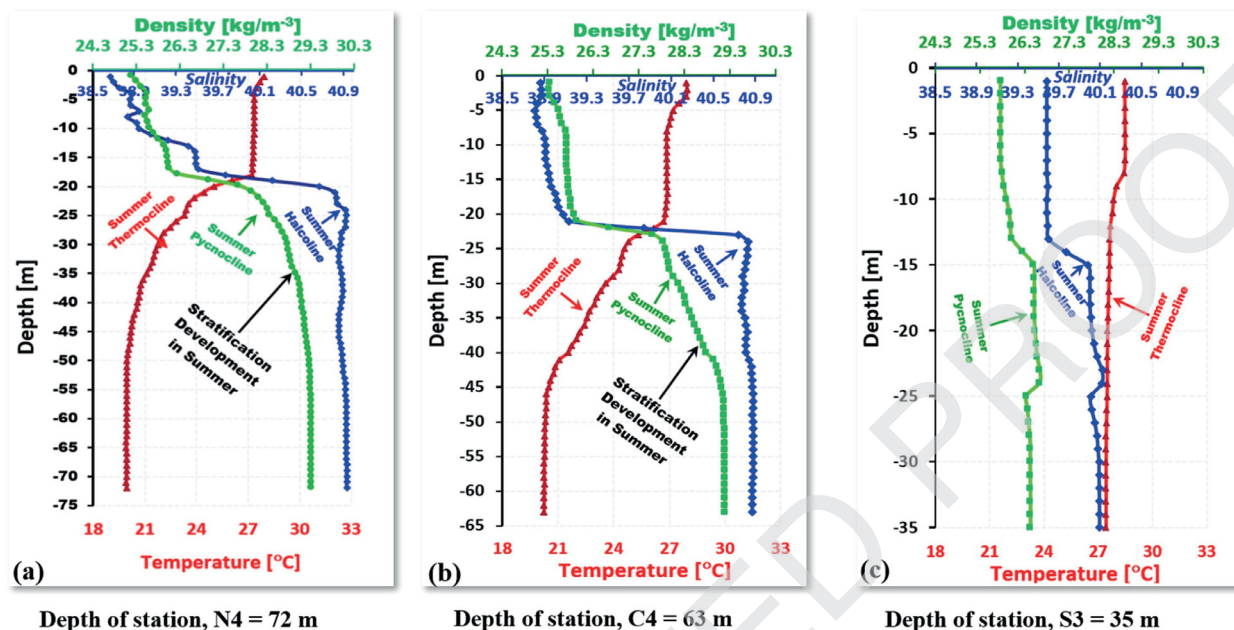


Figure 4 Vertical profiles of temperature, salinity and density at the deepest stations in the northern (a), central (b) and southern (c) transects. The plots are made using Microsoft Excel Data Analysis Tool.

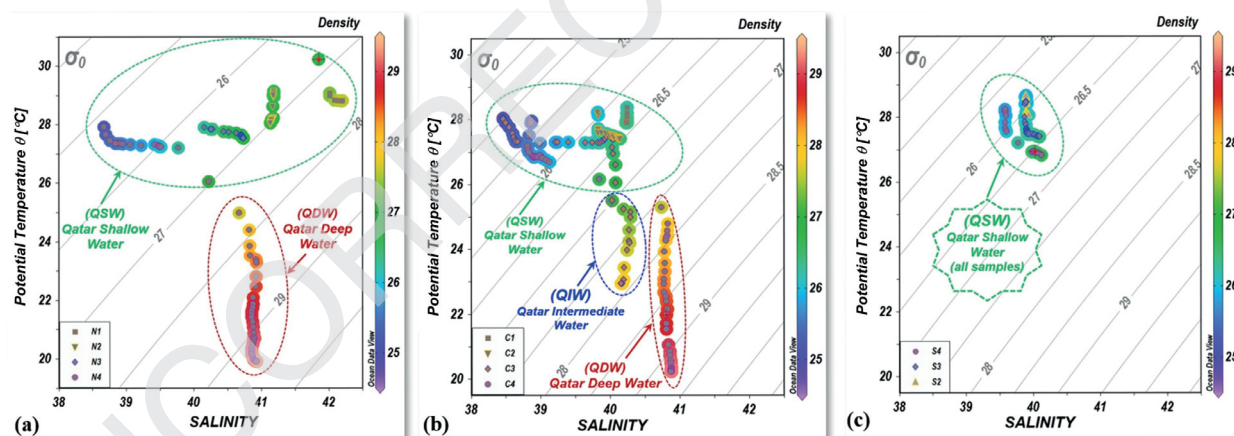


Figure 5 (a) Θ/S diagram derived from the measurements during May 28-30, 2017: (a) Qatar Shallow Water (QSW) and Qatar Deep Water (QDW) identified at the deepest station (N4=72m) in northern transect, (b) Qatar Shallow Water (QSW), Qatar Intermediate Water (QIW) and Qatar Deep Water (QDW) identified at the deepest station (C4=67m) in central transect and (c) Qatar Shallow Water (QSW) identified in the southern transect. The plots are made using Ocean Data View Software, Version 5.03, (Schlitzer, 2020).

Table 1 The physicochemical parameters in the composite water masses in the study area: Qatar Central Arabian Gulf Water (QCAGW) and their comparison with those in the Kuwait Coastal Waters (KCW), Northern Gulf Waters (NGW), Central Arabian Coastal Waters (CACW) and Indian Ocean Surface Water (IOSW) (after Al-Said et al., 2018).

Parameters	KCW*	NGW*	CACW*	IOSW*	QCAGW (present study)
Temperature (°C)	32.4–32.8	32.8–34.0	33.9–34.6	32.7–35.4	19.9–30.23
Salinity	40.8–41.1	39.2–40.7	38.1–39.9	38.8–40.2	38.46–42.20
DO (ml/l)	4.8–5.1	4.7–5.3	4.0–5.8	4.5–5.3	3.43–8.37
pH	7.9–7.9	7.7–8.0	8.0–8.2	7.7–8.1	4.3–8.21

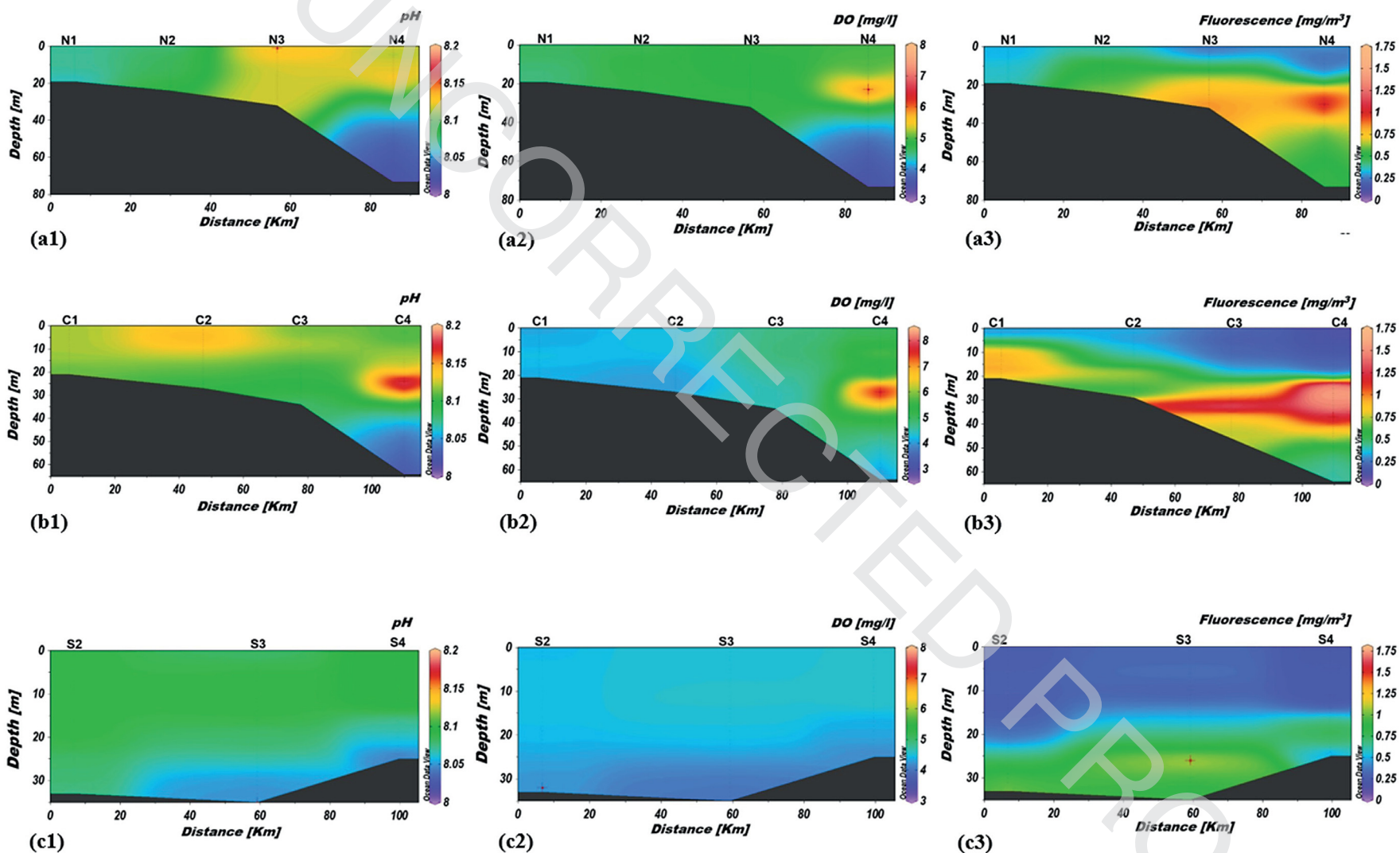


Figure 6 2D profiles of the measured pH (a1, b1, c1), DO (a2, b2, c2) and fluorescence (mg/m^3) (a3, b3, c3) along the northern central and southern transects. The plots are made using Ocean Data View Software, Version 5.03 (Schlitzer, 2020).

Table 2 Correlation matrix derived for the physicochemical parameters of northern, central and southern transects; ^apositive correlation significant at $p=0.01$, ^bpositive correlation significant at $p=0.05$, ^cnegative correlation significant at $p=0.01$ and ^dnegative correlation significant at $p=0.05$ (only significant correlations are given).

Transects	Parameters	Temperature (°C)	Salinity	Density (kg/m ³)	pH	DO (mg/l)	Fluorescence (mg/m ³)
Northern	Depth (m)	-0.91 ^c		0.86 ^a	-0.70 ^c	-0.59 ^c	0.28 ^a
	Temperature (°C)			-0.87 ^c	0.58 ^a	0.38 ^a	-0.36 ^c
	Salinity		0.47 ^a		-0.46 ^c	-0.20 ^d	0.17 ^b
	Density (kg/m ³)				-0.74 ^c	-0.43 ^c	0.41 ^a
	pH					0.81 ^a	
	DO (mg/l)						
	Fluorescence (mg/m ³)						
Central	Depth (m)	-0.92 ^c	0.72 ^a	0.91 ^a	-0.70 ^c		0.37 ^a
	Temperature (°C)		-0.67 ^c	-0.95 ^c	0.63 ^a	0.17 ^b	-0.31 ^c
	Salinity			0.87 ^a	-0.30 ^c		0.66 ^b
	Density (kg/m ³)				-0.53 ^c		0.50 ^a
	pH					0.52 ^a	
	DO (mg/l)						0.50 ^a
	Fluorescence (mg/m ³)						
Southern	Depth (m)	-0.58 ^c	0.63 ^a	0.70 ^a	-0.74 ^c	-0.83 ^c	0.86 ^a
	Temperature (°C)		-0.43 ^c	-0.91 ^c	0.65 ^a	0.43 ^a	-0.56 ^c
	Salinity			0.76 ^a	-0.83 ^c	-0.73 ^c	0.65 ^a
	Density (kg/m ³)				-0.84 ^c	-0.64 ^c	0.70 ^a
	pH					0.90 ^a	-0.77 ^c
	DO (mg/l)						-0.81 ^c
	Fluorescence (mg/m ³)						

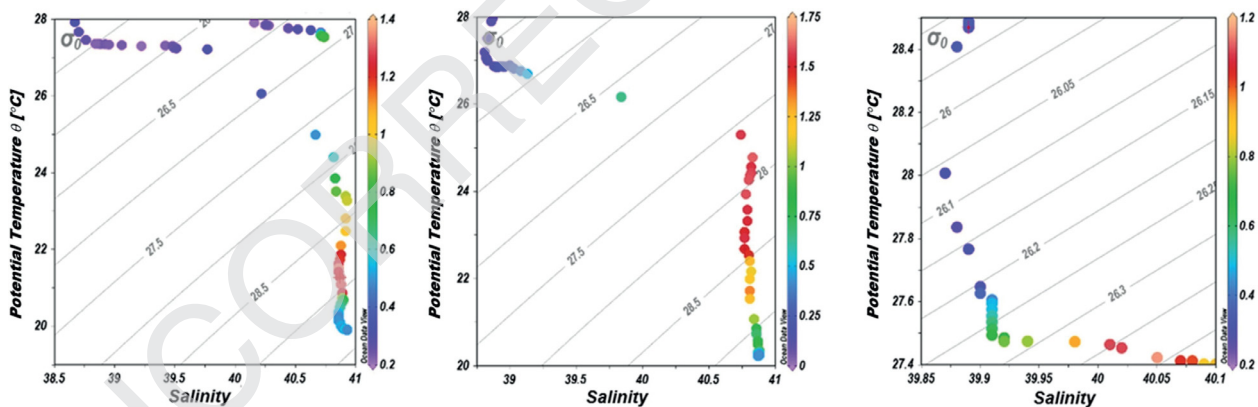


Figure 7 Fluorescence profiles along the northern (a), central (b) and southern (c) transects, indicating the most productive zone associated with high values of fluorescence. In the potential temperature-salinity-fluorescence plots, high values are shown in yellow and red colors.

304 transects (8.01–8.21) are well within the acceptable limits
 305 of the oceanic waters, where the average pH of seawater
 306 could be around 8.1 (Fallatah et al., 2018).

307 DO varies between 3 and 7 mg/l in the northern transect
 308 and between 3.5 and 8.5 mg/l in the central transect,
 309 while the southern transect has no significant variation,
 310 which is between 4.0 and 4.6 mg/l (Figure 6a2, b2,
 311 c2). The highest DO is found in the subsurface layer (20–30
 312 m) in the deep-water locations of the northern and central
 313 transects. This indicates that the subsurface layer in the
 314 QEEZ is well oxygenated during early summer. Earlier studies
 315 reported hypoxia at a depth of 60 m in the central Gulf
 316 in the mid/late summer developed by summer stratification
 317 (Al-Ansari et al., 2015; Rakib et al., 2021). However, the

318 minimum recorded DO in early summer in the present study
 319 is 3.43 mg/l, quite a comfortable situation compared to hy-
 320 hypoxic conditions in the later stage. This shows that the Gulf
 321 is still relatively healthy, despite several coastal develop-
 322 ment activities in the last few decades.

323 The Chlorophyll Fluorescence parameter (F_o) is used as a
 324 tracer in biological studies to estimate the primary produc-
 325 tivity (Chen et al., 2017). Distinct variation in fluores-
 326 cence is identified in all the transects (Figure 6a3, b3, c3).
 327 The surface layer of the deep-water locations has the lowest flu-
 328 orescence (0–0.2 mg/m³), while the subsurface layer (20–
 329 40 m) produces the highest fluorescence (1.0–1.6 mg/m³).
 330 Overall, the central transect is characterized by high fluo-
 331 rescence and thus high primary productivity. The northern

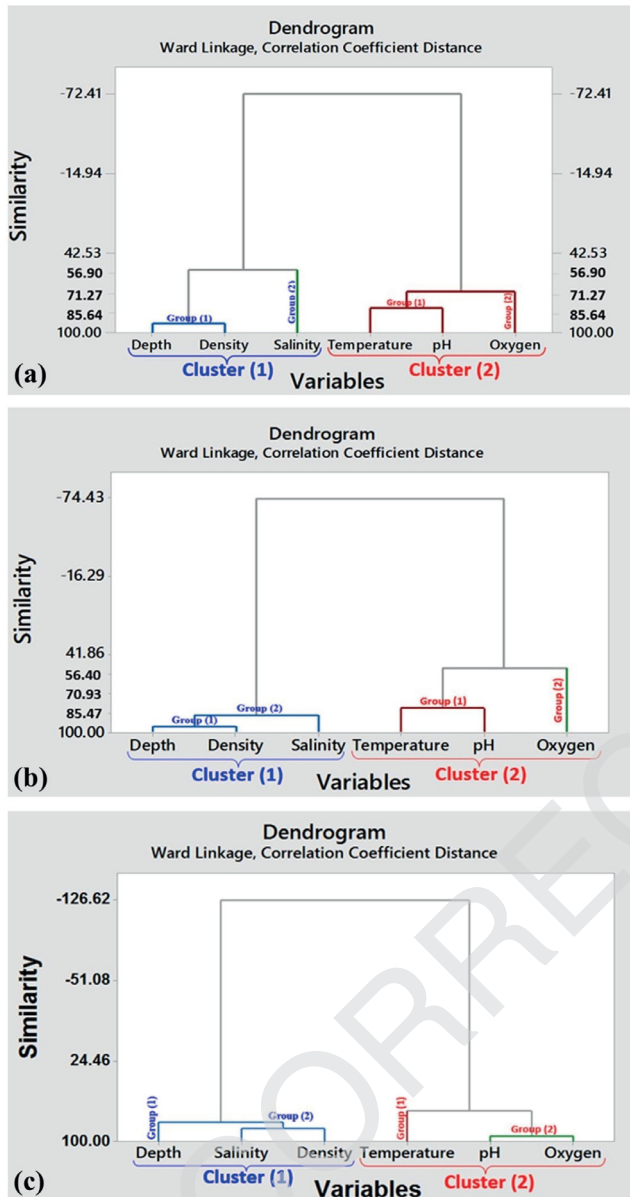


Figure 8 Hierarchical cluster analysis (HCA) of the physicochemical parameters in the: (a) northern transect, (b) central transect and (c) southern transect. (Dendrograms are made using Minitab Software Version 17).

332 transect also has a wide range of primary productive zone
 333 with reasonably high fluorescence, but relatively low compared
 334 to the central transect.

335 The higher fluorescence values are associated with a potential
 336 density of 28.100–29.020 and 27.590–29.000 kg/m³,
 337 respectively as shown in the northern and central transects,
 338 while Fo is associated with a lower potential density of
 339 26.320–26.427 kg/m³ in the southern transect (Figure 7a,
 340 b, c). The salinity associated with the higher fluorescence
 341 is around 40.8 in the northern and central transects, while
 342 that is around 40.0 in the southern transect. The temperature
 343 associated with higher fluorescence is 20.5–22.5°C,
 344 21.0–25.5°C and 27.4–27.5°C, respectively in the northern,
 345 central and southern transects. The central transect

has a wider range of temperature variations in the productive
 zone compared to the other two transects.

4.4. Correlation matrix between the physicochemical parameters

The statistical relationship between the physicochemical key parameters has been analyzed using the correlation matrix (Table 2) as well as the dendrograms (Figure 8). A higher positive correlation is found between density and depth in all the transects, which is quite common in oceanic waters. The depth versus salinity as well as density versus salinity has a strong positive correlation in the central and southern transects. This may be because of the sinking of high salinity water and the formation of dense bottom water; however, more in situ observations are needed to substantiate this feature. High negative correlations are found between the depth and temperature as well as density versus temperature in all transects. Although it is normal in oceanic waters, such a high correlation within the shallower depths of the Gulf is notable. The pH versus DO in the northern and southern transects, and pH versus temperature in the central and southern transects have high positive correlations. The pH has negative correlations with depth and density in all the transects, but within the shorter and normal range of pH (8.01–8.21), the shallow QEEZ does not yield any harmful impacts. The DO versus salinity has a strong negative correlation in the southern transect, within the limited data points. In the southern transect, the fluorescence has a strong positive correlation with depth, salinity and density. It suggests that although the salinity and density increase with depth, the reasonable amount of fluorescence (above 1.0 mg/m³) present in this region supports the primary productivity.

The hierarchical cluster analysis (HCA) produces the similarity percentage between the physicochemical parameters at each transect, which is represented by dendrograms (Figure 8). In the northern transect, the cluster (1) consists of depth, density and salinity, in which depth and density have high similarity (85%), whereas the cluster (2) consists of temperature, pH and DO, in which the temperature and DO have high similarity (75%) (Figure 8a). However, clusters (1) and (2) mutually exhibit a high negative similarity (–70%) in the northern transect. In the central and southern transects, the cluster components remain the same but differ in their similarity index compared to that in the northern transect. In the central transect, the depth and density in the cluster (1) have very high similarity (around 95%), indicating that density increases with depth, as reflected in the profiles, while both together show high similarity with salinity (around 85%) (Figure 8b). In the cluster (2), the temperature and pH show high similarity (around 80%). Similar to the northern transect, the clusters (1) and (2) in the central transect produce a high negative similarity (around –70%). In the southern transect, the density and salinity in the cluster (1) and pH and temperature in cluster (2) show high similarities (80% and 90%, respectively) (Figure 8c). The clusters (1) and (2) are mutually in a moderate negative similarity (–65%). These similarities suggest that salinity and density in the QEEZ are directly proportional to each other and have strong link between them, while both are inversely

405 proportional to temperature and pH. Furthermore, density
406 is more or less independent of temperature and pH, and
407 salinity determines the water column density and stability.

408 5. Summary and conclusions

409 This study investigated the spatial variability of key physicochemical parameters – temperature, salinity, density, pH, DO and fluorescence, in the Qatar's Exclusive Economic Zone (QEEZ) during early summer. There were 11 sampling stations across 3 transects – northern, central and southern. The results indicate that physicochemical parameters show distinct spatial variability, which is connected to the stratification and formation of different water masses in the QEEZ. The variations in temperature, salinity and potential density are in the range 19.9°–30.2°C, 38.46–42.20, 24.98–29.32 kg/m³, respectively. The minimum recorded salinity was in the intermediate region of the central transect, while the maximum recorded salinity was in the nearshore region of the northern transect. The higher salinity in the northern transect is primarily attributed to the higher evaporation rates along with dense water flow from the northern Gulf. Although not well-established, detailed investigations are required to evaluate the relative contribution of desalination plants in the hypersalinity of this region.

428 The pH in all the transects shows a little spatial variation (in the range of 8.01–8.21). Although small, the variations in pH are consistent with the water mass distributions, especially in the deep-water regions of northern and central transects. The DO was minimum (3.43 mg/l) in the deepest region of the northern transect, and maximum (8.37 mg/l) in the deepest region of the central transect. The summer stratification often leads to hypoxia in the central Gulf as literature reports, however, that is not quite evident in early summer based on the present study. The maximum recorded fluorescence was 1.61 mg/m³ in the deepest region of the northern transect. The high fluorescence in the QEEZ was confined to a depth of 20–40 m, where the primary productivity was relatively higher.

442 The northern and the central transects are situated in the deep-water zone and exhibited similar vertical and horizontal distribution patterns and layering of physicochemical key parameters, whereas the southern transect is situated in a relatively shallow water zone, exhibiting weak stratification. The correlation matrix and hierarchical cluster analysis indicate that depth, salinity and density are in cluster 1 and pH, DO and Temperature are in cluster 2, and both are inversely correlated to each other. The inferences derived in this study are preliminary in nature due to a limited number of datasets available in the QEEZ. A detailed investigation is planned by executing further measurements in the QEEZ, not only in summer but also in other seasons with the aim of studying the temporal variability of physicochemical parameters.

Q2 457 Uncited References

458 Allsop and Yao, 2010

Acknowledgments

This research was carried out as a part of the mission of the Environmental Science Center (ESC), Qatar University. The multipurpose research vessel, R.V Janan was utilized for data collection and sampling. The authors thank Prof. Hamad A. Al Saad, Director, ESC for his encouragement, keenness and continuous support. We thank Dr. Ahmed Saif Ibrahim for providing useful suggestions. We thank the sediment-focused research group and Mr. Mehmet Demirel for their assistance in data collection and analyses. Part of this work has been completed under the IRCC project (No. IRCC-2019-002).

Competing Interest

The authors of this study would like to declare that they have no conflict of interest.

Disclaimer

The manuscript contents are solely the responsibility of the authors, and do not necessarily represent the official views of the Qatar University and the Environmental Science Center (ESC).

CRedit Authorship contribution statements

Elnaiem Ali Elobaid: Conceptualization, research methodology, project administration, collection of samples, investigation, formal analysis, visualization, resources, writing the original draft of the manuscript, reviewing and editing.

Ebrahim S. Al Ansari: Conceptualization, methodology, project administration, resources, visualization, writing up, reviewing, and editing.

Oguz Yigiterhan: Conceptualization, research methodology, collection of samples methodology, resources, visualization, writing, reviewing, and editing.

V.M. Aboobacker: Conceptualization, research methodology, writing, reviewing, and editing.

P. Vethamony: reviewing and editing.

Supplementary materials

Supplementary material associated with this article can be found, in the online version, at doi:10.1016/j.oceano.2021.09.003.

References

- Abdel-Moati, M.A.R., Al-Ansari, I.S., 2000. Impact of the Expansion in Fertilizer Industry on the Levels of Ammonia and Urea of Mes-saieed Marine Area (Qatar), Arabian Gulf. *Fresenius Envir. Bull.* 9, 040–046. <https://doi.org/10.1029/92JC00841>.
- Aboobacker, V.M., Shanas, P.R., Veerasingam, S., Ibrahim M.A.S. Al-Ansari, Fadhil N Sadooni, Vethamony, P., 2021a. Long-term

- assessment of onshore and offshore wind energy potentials of Qatar, *Energies* 14, 1178. <https://doi.org/10.3390/en14041178>
- Aboobacker, V.M., Shanass, P.R., Al-Ansari, E.M.A.S., Sanil Kumar, V., Vethamony, P., 2021b. The maxima in northerly wind speeds and wave heights over the Arabian Sea, the Arabian/Persian Gulf and the Red Sea derived from 40 years of ERA5 data. *Clim. Dyn.* 56, 1037–1052. <https://doi.org/10.1007/s00382-020-05518-6>.
- Al-Ansari, E.M.A.S., Rowe, G., Abdel-Moati, M.A.R., Yigiterhan, O., Al-Maslamani, I., Al-Yafei, M.A., Al-Shaikh, I., Upstill-Goddard, R., 2015. Hypoxia in the central Arabian Gulf Exclusive Economic Zone (EEZ) of Qatar during summer season. *Estuar. Coast. Shelf Sci.* 159, 60–68. <https://doi.org/10.1016/j.ecss.2015.03.022>.
- Al-Ansari, I.M.A.S., 2006. A hydrographic and biogeochemical study of waters and sediment of the exclusive economic zone (EEZ) of Qatar (Arabian Gulf) Ph.D. thesis. the University of Newcastle upon Tyne, UK.
- Al Azhar, M., Temimi, M., Zhao, J., Ghedira, H., 2016. Modeling of circulation in the Arabian Gulf and the Sea of Oman: Skill assessment and seasonal thermohaline structure. *J. Geophys. Res. Oceans* 121, 1700–1720. <https://doi.org/10.1002/2015JC011038>.
- Allsop, N.K., Yao, F., 2010. Experiences of hybrid Ocean modelling of the Persian Gulf on the Blue Gene/P*. Available at http://www.hpc.kaust.edu.sa/events/Supercomputing_44__November_2010/posters/KAUST_NKA_SC10.pdf
- Al-Majed, N., Mohammadi, H., Al-Ghadban, A., 2000. Regional Report of the State of the Marine Environment. ROPME/GX-10/001/1. Revised by Al-Awadi A., Regional Organization for the Protection of the Marine Environment. Available at http://www.ropme.org/Uploads/SOMER/SOMER_2000.pdf
- Al-Said, T., Yamamoto, Madhusoodhanan, R., Al-Yamani, F., Pokavanich, T., 2018. Summer hydrographic characteristics in the northern ROPME Sea Area: Role of ocean circulation and water masses. *Estuar. Coast. Shelf Sci.* 213, 18–27. <https://doi.org/10.1016/j.ecss.2018.07.026>.
- Beltagy, A.I., 1983. Some oceanographic measurements in the Gulf waters around Qatar Peninsula. *Qatar Univ. Sci. Bull.* 3, 329–341.
- BP, 2011. Statistical Review of World Energy, June 2011. London SW1 Y 4PD, UK sr@bp.com
- Brewer, P.G., Dyrssen, D., 1985. Chemical oceanography of the Persian Gulf. *Prog. Oceanogr.* 14, 41–55. [https://doi.org/10.1016/0079-6611\(85\)90004-7](https://doi.org/10.1016/0079-6611(85)90004-7).
- Campos, E.J.D., Gordon, A.L., Kjerfve, B., Vieira, F., Cavalcante, G., 2020. Freshwater budget in the Persian (Arabian) Gulf and exchanges at the Strait of Hormuz. *PLoS ONE* 15 (5), e0233090. <https://doi.org/10.1371/journal.pone.0233090>.
- Chao, S.Y., Kao, T.W., Al-Hajri, K.R., 1992. A numerical investigation of circulation in the Arabian Gulf. *J. Geophys. Res.* 97 (C7), 11219–11236. <https://doi.org/10.1029/92JC00841>, Available at.
- Chen, H., Zhou, W., Chen, W., Xie, W., Jiang, L., Liang, Q., Huang, M., Wu, Z., Wang, Q., 2017. Simplified, rapid, and inexpensive estimation of water primary productivity based on chlorophyll fluorescence parameter *Fo*. *J. Plant Physiol.* 211, 128–135. <https://doi.org/10.1016/j.jplph.2016.12.015>.
- Emery, K.O., 1956. Sediments and Water of the Persian Gulf. *AAPG Bull.* 40, 2354–2383. <https://doi.org/10.1306/5CEAE595-16BB-11D7-8645000102C1865D>.
- Fallatah, M.M., Kavil, Y.N., Ibrahim, A.S.A., Orif, M.I., Shaban, Y.A., Al Farawati, R., 2018. Hydrographic parameters and distribution of dissolved Cu, Ni, Zn and nutrients near Jeddah desalination plant. *Open Chem* 16, 245–257. <https://doi.org/10.1515/chem-2018-0029>.
- Fofonoff, N.P., Millard, R.C., 1983. Algorithms for the computation of fundamental properties of seawater. *UNESCO Tech. Papers Marine Sci.* 44, 53. <http://hdl.handle.net/11329/109>.
- Ghaemi, M., Abtahi, B., Gholampour, S., 2021. Spatial distribution of nutrients and chlorophyll a across the Persian Gulf and the Gulf of Oman. *Ocean Coast. Manage.* 201, 105476. <https://doi.org/10.1016/j.ocecoaman.2020.105476>.
- Hunter, J.R., 1986. The physical oceanography of the Arabian Gulf: a review and theoretical interpretation of previous observations. In: Halwagy, R., Clyton, D., Behbehani, M. (Eds.), *First Arabian Gulf Conference on Environment and Pollution*. Kuwait, February 7–9, 1982. University of Kuwait, 1–23.
- Ibrahim, H.D., Xue, P., Eltahir, E.A., 2020. Multiple Salinity Equilibrium and Resilience of Persian/Arabian Gulf Basin Salinity to Brine Discharge. *Front. Marine Sci.* 7, 573. <https://doi.org/10.3389/fmars.2020.00573>.
- Ibrahim, H.D., Eltahir, E.A., 2019. Impact of brine discharge from seawater desalination plants on persian/arabian gulf salinity. *J. Environ. Eng.* 145, 04019084. [https://doi.org/10.1061/\(ASCE\)EE.1943-7870.0001604](https://doi.org/10.1061/(ASCE)EE.1943-7870.0001604).
- John, V.C., Coles, S.L., Abozed, A.I., 1990. Seasonal cycles of temperature, salinity and water masses of the western Arabian Gulf. *Oceanologica Acta* 13, 273–282.
- Jones, D.A., Price, A.R.G., Al-Yamani, F., Al-Zaidan, A., 2002. Coastal and marine ecology. In: Khan, N.Y., Munawar, M., Price, A.R.G. (Eds.), *The Gulf Ecosystem: Health and Sustainability*. Backhuys Publishers, Leiden, 65–103. <https://doi.org/10.14321/J.CTT1TM7JKG.12>.
- Joydas, T.V., Qurban, M.A., Manikandan, K.P., Ashraf, T.T.M., Ali, S.M., Al-Abdulkader, K., Qasem, A., Krishnakumar, P.K., 2015. Status of macrobenthic communities in the hypersaline waters of the Gulf of Salwa, Arabian Gulf. *J. Sea Res.* 99, 34–46. <https://doi.org/10.1016/j.seares.2015.01.006>.
- Kampf, J., Sadrasab, M., 2006. The circulation of the Persian Gulf: a numerical study. *Ocean Sci* 2, 27–41. <https://doi.org/10.5194/os-2-27>.
- Ma, X., Zuo, H., Tian, M., Zhang, L., Meng, J., Zhou, X., Min, N., Chang, X., Liu, Y., 2016. Assessment of heavy metals contamination in sediments from three adjacent regions of the Yellow River using metal chemical fractions and multivariate analysis techniques. *Chemosphere* 144, 264–272. <https://doi.org/10.1016/j.chemosphere.2015.08.026>.
- Pous, S., Pascal, L., Xavier, C., 2015. A model of the general circulation in the Persian Gulf and in the Strait of Hormuz: Intraseasonal to interannual variability. *Cont. Shelf Res.* 94, 55–70. <https://doi.org/10.1016/j.csr.2014.12.008>.
- Prasad, T.G., Ikeda, M., Prasanna Kumar, S., 2001. Seasonal spreading of the Persian Gulf Water mass in the Arabian Sea. *J. Geophys. Res.* 106 (C8), 17059–17071. <https://doi.org/10.1029/2000JC000480>.
- Price, A., 2002. Simultaneous hotspots and coldspots of the marine biodiversity and the implications for global conservation. *Mar. Ecol. Prog. Ser.* 241, 23–27. <https://doi.org/10.3354/meps241023>.
- Privett, D.W., 1959. Monthly charts of evaporation from the N. Indian Ocean (including the Red Sea and the Persian Gulf). *Q. J. Roy. Meteor. Soc.* 85, 424–428. <https://doi.org/10.1002/qj.49708536614>.
- Rakib, F., Al-Ansari, E.M.A.S., Husrevoglu, Y.S., Yigiterhan, O., Al-Maslamani, I., Aboobacker, V.M., Vethamony, P., 2021. Observed variability in physical and biogeochemical parameters in the central Arabian Gulf. *Oceanologia* 63 (2), 227–237. <https://doi.org/10.1016/j.oceano.2020.12.003>.
- Reynolds, M., 1993. Physical oceanography of the Gulf, Strait of Hormuz and Gulf of Oman: results from the Mt. Mitchell expedition. *Mar. Pollut. Bull.* 27, 35–59. [https://doi.org/10.1016/0025-326X\(93\)90007-7](https://doi.org/10.1016/0025-326X(93)90007-7).
- Reynolds, R.M., 2002. Oceanography. In: Khan, N.Y., Munawar, M., Price, A.R.G. (Eds.), *The Gulf Ecosystem: Health and Sustainability*. Backhuys Publishers, Leiden, 53–64.
- Rivers, J.M., Varghese, L., Yousif, R., Whitaker, F.F., Skeat, S.L., Al-

- 640 Shaikh, I., 2019. The geochemistry of Qatar coastal waters and
641 its impact on carbonate sediment chemistry and early marine
642 diagenesis. *J. Sediment. Res.* 89, 293–309. <https://doi.org/10.2110/jsr.2019.17>.
- 643 Schlitzer, R., 2020. Ocean Data View Latest ODV Version: ODV 5.3.0
644 (June 03 2020). Germany.
- 645 Sezer, N., Evis, Z., Koc, M., 2017. Management of Desalination Brine
646 in Qatar and the GCC Countries. In: 10th International Confer-
647 ence on Sustainable Energy and Environmental protection (June
648 27th–30th, 2017, Bled, Slovenia). University of Maribor Press
649 <https://doi.org/10.18690/978-961-286-053-0.11>.
- 650 Sheppard, C.R.C., 1993. Physical environment of the Gulf relevant
651 to marine pollution: An overview. *Mar. Pollut. Bull.* 27, 3–8.
652 [https://doi.org/10.1016/0025-326X\(93\)90003-3](https://doi.org/10.1016/0025-326X(93)90003-3).
- 653 Sheppard, C., Al-Husiani, M., Al-Jamali, F., Al-Yamani, F., Bald-
654 win, R., Bishop, J., Benzoni, F., Dutrieux, E., Dulvy, N.K., Durva-
655 sula, S.R.V., Jones, D.A., Loughland, R., Medio, D., Nithyanan-
656 dan, M., Pilling, G.M., Polikarpov, I., Price, A.R.G., Purkis, S.,
657 Riegl, B., Saburova, M., Namin, K.S., Taylor, O., Wilson, S.,
658 Zainal, K., 2010. The Gulf: A young sea in decline. *Mar. Pollut.*
659 *Bull.* 60, 13–38. <https://doi.org/10.1016/j.marpolbul.2009.10.017>.
- 660 Smith, R., Purnama, A., Al-Barwani, H.H., 2007. Sensitivity of hy-
661 persaline Arabian Gulf to seawater desalination plants. *Appl.*
662 *Math. Model.* 31, 2347–2354. <https://doi.org/10.1016/j.apm.2006.09.010>.
- 663 Soliman, Y.S., Alansari, E.M.A., Sericano, J.L., Wade, T.L., 2019.
664 Spatio-temporal distribution and sources identifications of poly-
665 cyclic aromatic hydrocarbons and their alkyl homolog in surface
666 sediments in the central Arabian Gulf. *Sci. Total Environ.* 658,
667 787–797. <https://doi.org/10.1016/j.scitotenv.2018.12.093>.
- 668 Swift, S.A., Bower, A.S., 2003. Formation and circulation of dense
669 water in the Persian/Arabian Gulf. *J. Geophys. Res.* 108.
670 <https://doi.org/10.1029/2002jc001360>, 4-1–4-21.
- 671 Thoppil, P.G., Hogan, P.J., 2010. Persian Gulf response to a win-
672 tertime shamal wind event. *Deep Sea Res. Pt. I* 57, 946–955.
673 <https://doi.org/10.1016/j.dsr.2010.03.002>.
- 674 Van Lavieren, H., Burt, J., Feary, D.A., Cavalcante, G., Marquis, E.,
675 Benedetti, L., Trick, C., Kjerfve, B., Sale, P.F., 2011. Managing
676 the growing impacts of development on fragile coastal and ma-
677 rine ecosystems: Lessons from the Gulf. UNU-INWEH, Hamilton,
678 ON, Canada, 100 Policy Report.
- 679 Vasou, P., Vervatis, V., Krokos, G., Hoteit, I., Sofianos, S., 2020.
680 Variability of water exchanges through the Strait of Hor-
681 muz. *Ocean Dynam* 70, 1053–1065. <https://doi.org/10.1007/s10236-020-01384-2>.
- 682 Yao, F., Johns, W.E., 2010. A HYCOM modeling study of the
683 Persian Gulf:1. Model configurations and surface circula-
684 tion. *J. Geophys. Res.* 115, C11017. <https://doi.org/10.1029/2009JC005781>.
- 685 Yoshida, J., Matsuymn, M., Senjyu, T., Ishimaru, T., Mopingaga, T.,
686 Arakwa, H., Kamatani, A., Maeda, M., Otsuki, A., Hashimoto, S.,
687 Kasuga, I., Koike, Y., Mine, Y., Kurita, Y., Kitazawa, A., Noda, A.,
688 Hayashi, T., Miyazaki, T., Takahashi, K., 1998. Hydrography in
689 the RSA during the RT/V Umitaka-Maru cruises. In: Otsuki, A.,
690 Abdeulraheem, M., Reynolds, M. (Eds.), *Offshore Environment of
691 the ROPME Sea Area after the War-Related Oil Spill – Results
692 of the 1993–94 Umitaka-Maru Cruise*. Terra Sci. Publ. Company,
693 Tokyo, 1–22.